Journal of Photochemistry and Photobiology A: Chemistry 200 (2008) 396–401

Contents lists available at ScienceDirect

Journal of Photochemistry and Photobiology A: Chemistry

journal homepage: www.elsevier.com/locate/jphotochem

Photosensitizing properties of octacarboxy metallophthalocyanines in aqueous medium and their interaction with bovine serum albumin

Mopelola Idowu, Tebello Nyokong*

Department of Chemistry, Rhodes University, Grahamstown 6140, South Africa

ARTICLE INFO

Article history:
Received 26 May 2008
Received in revised form 2 September 2008
Accepted 4 September 2008
Available online 18 September 2008

Keywords:
Phthalocyanine
Bovine serum albumin
Stern–Volmer
Triplet yield
Triplet lifetime
Fluorescence quenching

ABSTRACT

Photosensitizing properties of aluminium, silicon, zinc and germanium octacarboxy phthalocyanines ((OH)AlOCPc, $(OH)_2$SiOCPc, ZnOCPc and $(OH)_2$GeOCPc) were studied in aqueous medium and in the presence of bovine serum albumin (BSA). Triplet quantum yields increased with increasing atomic number of the central metals of the metallophthalocyanine. The efficiency of singlet oxygen generation via energy transfer from the excited triplet state of the octacarboxy metallophthalocyanines (MOCPcs) to ground state oxygen increased markedly in the presence of BSA. The triplet state lifetimes of the MOCPc complexes in the presence of BSA were found to be longer than in the absence of BSA, ranging from 110 to 580 μs. These complexes bind readily to BSA. Stern–Volmer quenching constant K_{SV} as well as the binding constant k_b values were calculated. The probable mechanism of quenching of BSA fluorescence by the MOCPc complexes is by static quenching.

1. Introduction

The application of metallophthalocyanines (MPcs) in oncology has significantly increased in the last few decades due to their interesting properties especially their efficacy in photodynamic therapy (PDT) of cancer [1–4]. PDT, which is an emerging modality for the treatment of a variety of cancers, is based on the concept of preferential accumulation of a photosensitizer in the target malignant tissue and application of a precise illumination, to provide the selectivity of the treatment. The light penetrates the tissue and causes excitation of the photosensitizer which transfers its triplet state energy to nearby oxygen molecules to form electronically excited and highly reactive singlet oxygen species, which causes cytotoxic reactions in the cells [4–7]. Incorporation of non-transition metals such as aluminium, silicon, zinc and germanium in the centre of the phthalocyanine (Pc) ring results in complexes with high triplet state quantum yields and long triplet lifetimes, which are required for efficient photosensitization [8]. MPcs are particularly interesting since anionic or cationic groups such as carboxylic, sulfonic or quaternized amino groups render them water-soluble [9,10]. This makes them very useful for PDT, which requires water solubility of the complexes for easy administration into the blood stream.

Serum albumins are major binding proteins for most drugs. As the major soluble protein constituents of the circulatory system, serum albumins play an important role in the transport of many exogenous and endogenous ligands, binding covalently or reversibly to these ligands and increasing the passive tumor selectivity of the drug by enhanced permeation and retention effect [11–13]. Therefore for many drugs, binding to serum albumin is an important determinant of their distribution and fate in the body [14].

The interaction of some MPc complexes with bovine serum albumin (BSA) has been reported [10,15–17]. Sulfonated MPcs (when in the non-aggregated form) showed a decrease in quantum yield of fluorescence (Φ_F) in the presence of BSA [17] and an increase in Φ_F when aggregated. The binding constants for the binding of $GePcS_{mix}$, $SiPcS_{mix}$, $SnPcS_{mix}$ and $ZnPcS_{mix}$ (containing a mixture of differently sulfonated MPc derivatives) to BSA were found to be of the order of 1×10^6 dm^3 mol^{-1} [17].

In this work, we report on the photophysical and photochemical properties of silicon, germanium, aluminium and zinc octacarboxy phthalocyanine (MOCPc) complexes (Fig. 1, inset) in aqueous medium. The association of the MOCPc complexes with bovine serum albumin is also studied. MOCPc complexes are water-soluble and are known to be monomeric in aqueous medium [18], thus are expected to give better photosensitizing properties compared to the sulfonated MPc complexes. ZnOCPc has been reported to give a singlet oxygen quantum yield (Φ_Δ) value of 0.52 [8]. For (OH)AlOCPc, association via hydrogen bonding occurs affecting the

* Corresponding author. Tel.: +27 46 6038260; fax: +27 46 6225109.
E-mail address: t.nyokong@ru.ac.za (T. Nyokong).

1010-6030/$ – see front matter © 2008 Elsevier B.V. All rights reserved.
doi:10.1016/j.jphotochem.2008.09.003

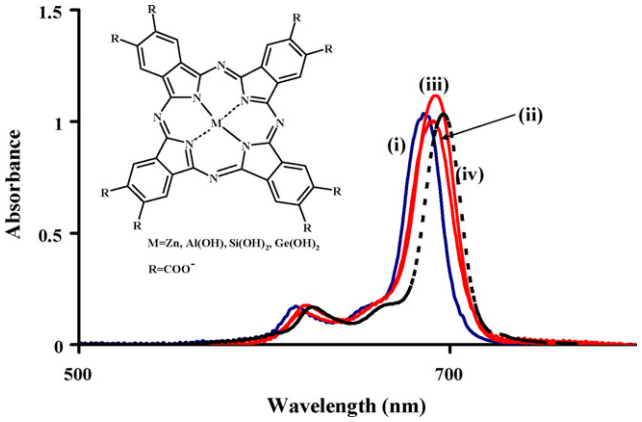

Fig. 1. Ground state electronic absorption spectra of the MPc carboxylate complexes in PBS pH 7.4; (i) (OH)AlOCPc, (ii) $(OH)_2$SiOCPc, (iii) ZnOCPc, (iv) $(OH)_2$GeOCPc. Concentration ~ 10^{-6} mol dm^{-3}. Inset: Chemical structures of octacarboxy substituted metallophthalocyanine.

production of singlet oxygen hence the photosensitizing ability [8]. There have been no reports on the photochemical and photophysical behavior of SiOCPc and GeOCPc derivatives.

2. Experimental

2.1. Materials

Aluminium, silicon, zinc and germanium octacarboxy phthalocyanines ((OH)AlOCPc, $(OH)_2$SiOCPc, ZnOCPc and $(OH)_2$GeOCPc) were synthesized, purified and characterized according to literature methods [19]. Zinc tetrasulfophthalocyanine ($ZnPcS_4$) and $ZnPcS_{mix}$ were also synthesized, purified and characterized according to literature methods [20,21] respectively. Bovine serum albumin and anthracene-9,10-bis-methylmalonate (ADMA) were obtained from Aldrich. Phosphate-buffered saline (PBS) solution (0.01 M, pH 7.4) was prepared using appropriate amounts of Na_2HPO_4, KH_2PO_4 and chloride salts, dissolved in ultra pure water from a Milli-Q Water System (Millipore Corp., Bedford, MA, USA).

2.2. Equipment

Fluorescence excitation and emission spectra were recorded on a Varian Eclipse spectrofluoremeter. UV–vis spectra were recorded on a Varian 500 UV–vis/NIR spectrophotometer. Laser flash photolysis experiments were performed with light pulses produced by a Quanta-Ray Nd:YAG laser providing 400 mJ, 90 ns pulses of laser light at 10 Hz, pumping a Lambda-Physik FL3002 dye (Pyridin 1 dye in methanol). Single pulse energy ranged from 2 to 7 mJ. The analyzing beam source was from a Thermo Oriel xenon arc lamp, and a photomultiplier tube was used as detector. Signals were recorded with a digital real-time oscilloscope (Tektronix TDS 360). The triplet life times were determined by exponential fitting of the kinetic curves using the program OriginPro 7.5. Photo-irradiations for photodegradation or singlet oxygen determination were performed using a General electric Quartz line lamp (300 W). A 600 nm glass cut off filter (Schott) and water were used to filter off ultraviolet and infrared radiations respectively. An interference filter (Intor, 670 nm with a band width of 40 nm) was additionally placed in the light path before the sample. Light intensity was measured with a POWER MAX5100 (Molelectron detector incorporated) power meter and was found to be 3.12×10^{16} photons s^{-1} cm^{-2} for photobleaching and to be 1.25×10^{16} photons s^{-1} cm^{-2} for singlet oxygen studies.

2.3. Photophysical and photochemical studies

Fluorescence quantum yields (Φ_F) were determined by comparative method [22] (Eq. (1)),

$$\Phi_F = \Phi_{F(Std)} \frac{FA_{Std}n^2}{F_{Std}An^2_{Std}} \quad (1)$$

where F and F_{Std} are the areas under the fluorescence curves of the MPc derivatives and the reference, respectively. A and A_{Std} are the absorbances of the sample and reference at the excitation wavelength, and n and n_{Std} are the refractive indices of solvents used for the sample and standard, respectively. ZnPc in DMSO was used as a standard, $\Phi_F = 0.2$ [23]. At least three independent experiments were performed for the quantum yield determinations. Both the sample and the standard were excited at the same relevant wavelength.

Triplet quantum yields were determined using a comparative method based on triplet decay, using Eq. (2):

$$\Phi_T^{Sample} = \Phi_T^{Std} \frac{\Delta A^{Sample} \varepsilon^{Std}}{\Delta A^{Std} \varepsilon^{Sample}} \quad (2)$$

where A_T^{Sample} and A_T^{Std} are the changes in the triplet state absorbance of the sample and the standard, respectively. ε_T^{Sample} and ε_T^{Std} are the triplet state extinction coefficients for the sample and standard, respectively. Φ_T^{Std} is the triplet state quantum yield for the standard. ZnTSPc in aqueous solution, $\Phi_T^{Std} = 0.56$ [24] was used as standard.

The values of photobleaching quantum yields (Φ_P) were determined using Eq. (4),

$$\Phi_{Pd} = \frac{(C_0 - C_t)VN_A}{I_{abs}St} \quad (4)$$

where C_t and C_0 are the MPc concentration in mol dm^{-3} after and prior to irradiation, respectively. V is the reaction volume, S is the irradiation area of the cell, t the irradiation time, N_A is the Avogadro's number and I_{abs} the overlap integral of the radiation light source intensity and the absorption of the MPc in the region of the interference filter transmittance [25]. Eq. (5) was employed for calculating singlet oxygen quantum yields:

$$\Phi_\Delta = \Phi_\Delta^{Std} \frac{R_{ADMA} I_{abs}^{Std}}{R_{ADMA}^{Std} I_{abs}} \quad (5)$$

where Φ_Δ^{Std} is the singlet oxygen quantum yield for the standard ($ZnPcS_{mix}$, $\Phi_\Delta^{Std} = 0.45$ in aqueous solution) [26]. R_{ADMA} and R_{ADMA}^{Std} are the ADMA photobleaching rates in the presence of the MOCPc derivatives under investigation and the standard respectively. I_{abs} and I_{abs}^{Std} are the rates of light absorption by the MPc derivatives and the standard, respectively. To avoid chain reactions, the concentration of ADMA was kept at ~6×10^{-5} mol l^{-1}. Solutions of the MPc derivatives with an absorbance of 0.2 at the irradiation wavelength were prepared in the dark and irradiated at the Q band region, monitoring the ADMA degradation at 380 nm. The error was ~10% from several values of Φ_Δ.

3. Results and discussion

3.1. Ground state electronic absorption and fluorescence spectra

Octacarboxy metallophthalocyanines (MOCPcs) complexes are known and the (OH)AlOCPc, ZnOCPc, $(OH)_2$SiOCPc and $(OH)_2$GeOCPc gave satisfactory spectroscopic analyses similar to literature [19].

Table 1
Spectral and photophysicochemical parameters for MPc complexes in aqueous solution. BSA:MOCPc (10:1).

Sample	λ_Q (nm)	log ε	λ_F (nm)	Φ_F (±0.01) λ_{exc} = 640 nm	Φ_T (±0.01)	Φ_Δ (±0.01)	S_Δ[a]	$\Phi_{Pd} \times 10^5$	τ_T (μs)
(OH)AlOCPc	689	5.26	694	0.27	0.32	0.12	0.38	0.26	450 ± 6
(OH)AlOCPc + BSA	688		706	0.25	0.28	0.29	1.04	3.01	580 ± 5
ZnOCPc	693	5.25	702	0.23	0.50	0.32	0.64	2.65	160 ± 2
ZnOCPc + BSA	695		709	0.21	0.43	0.40	0.93	7.01	280 ± 2
$(OH)_2$SiOCPc	691	5.10	703	0.24	0.34	0.22	0.65	86.3	90 ± 2
$(OH)_2$SiOCPc + BSA	689		705	0.21	0.36	0.26	0.72	93.2	110 ± 1
$(OH)_2$GeOCPc	697	5.15	704	0.13	0.62	0.31	0.51	2.12	240 ± 5
$(OH)_2$GeOCPc + BSA	700		708	0.12	0.58	0.40	0.69	5.21	300 ± 2

[a] $S_\Delta = \Phi_\Delta/\Phi_T$.

The ground state electronic absorption spectra of (OH)AlOCPc, ZnOCPc, $(OH)_2$SiOCPc and $(OH)_2$GeOCPc in PBS pH 7.4 (Fig. 1) show characteristic absorption in the Q band region at ~690 nm. The spectra of these MOCPcs showed monomeric behavior evident by a single narrow Q band typical of metallated phthalocyanine complexes [27]. MPc complexes are known to be aggregated in aqueous media. However the MOCPcs are water-soluble but are not aggregated in water as observed before [18]. Aggregation in MPc complexes is due to coplanar association of the rings. It is likely that the MOCPc derivatives are not aggregated due to the plurality of the substituents preventing coplanar association. The Q band positions of these complexes are relatively red shifted with increase in atomic number of the central metal, Table 1. Fluorescence excitation spectra of these complexes are similar to their absorption spectra and are mirror images of the fluorescence emission spectra which is usual for MPc derivatives as shown in Fig. 2 (for $(OH)_2$SiOCPc) with the Stokes' shift in the neighbourhood of 10 nm.

3.2. Photophysical and photochemical parameters

Φ_F values for the MOCPcs are listed in Table 1. Φ_F values decrease with increase in atomic number of the central metal and this observation is consistent with the strengths of spin–orbit (S–O) coupling induced by the respective central metals based on their relative atomic numbers. An aftermath of enhanced S–O coupling is the reduction in the likelihood of fluorescence.

Φ_T is the measure of the fraction of absorbing molecules that undergo intersystem crossing (isc) to the triplet state. The efficiency of a phthalocyanine as a photosensitizer is determined by its triplet state quantum yield (Φ_T) and lifetime (τ_T). The variation of Φ_T among the complexes in Table 1 depended on heavy atom effect which encourages intersystem crossing to the triplet state. The observed trend for Φ_T corresponds to the increase in atomic number of the central metals, with the aluminium and silicon complexes having lower values compared to zinc and germanium MOCPcs in which the central metals have higher atomic numbers. The triplet lifetime, τ_T values range from 90 to 450 μs, which is a usual range for many MPc complexes. It is expected that central metals with high atomic numbers and diamagnetic properties will exhibit high Φ_T values and short τ_T values. Indeed in Table 1 (OH)AlOCPc with the lowest Φ_T has the longest triplet lifetime, however $(OH)_2$SiOCPc with Φ_T = 0.34 has a shorter triplet lifetime (90 μs) compared to $(OH)_2$GeOCPc with Φ_T = 0.62 and τ_T = 240 μs.

The presence of molecular oxygen is essential for the phototoxicity of phthalocyanines since photosensitized oxidation is the accepted chemical mechanism for photodynamic therapy. There is a necessity of high efficiency of transfer of energy between excited triplet state of MPc and ground state of oxygen to generate large amounts of singlet oxygen. The Φ_Δ values (Table 1) are higher for the MOCPc complexes with the higher Φ_T values. An efficient production of singlet oxygen was observed with S_Δ (=Φ_Δ/Φ_T), the efficiency of quenching of the triplet excited state by oxygen, being near unity (Table 1) with the exception of (OH)AlOCPc and $(OH)_2$GeOCPc in the absence of BSA.

Degradation of the molecules under irradiation can be used to study their stability. From Table 1, $(OH)_2$SiOCPc was found to be the least stable under irradiation while (OH)AlOCPc was found to be the most stable. In general, all the complexes are stable under irradiation for photosensitized reactions to occur. The low Φ_Δ values are reflected in the photodegradation values of (OH)AlOCPc and $(OH)_2$GeOCPc since they both exhibit the lowest photodegradation values. This may have been possible since photodegradation process is believed to be singlet oxygen mediated [28]. $(OH)_2$SiOCPc behaved differently both alone and in the presence of BSA in that its rate of photodegradation does not correlate to its singlet oxygen generation.

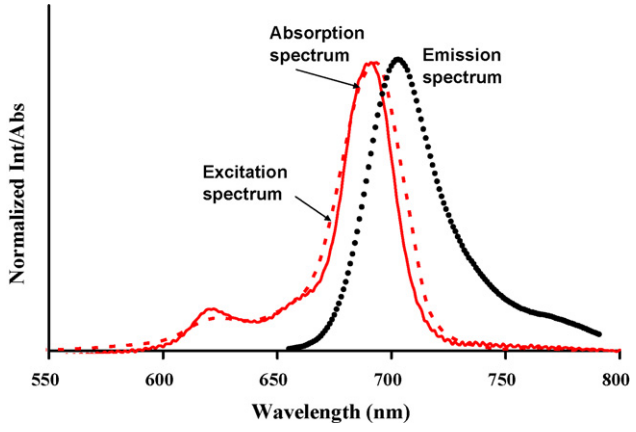

Fig. 2. Absorption (solid line) excitation (dashed line) and emission (dotted line) spectra of $(OH)_2$SiOCPc (λ_{exc} = 640 nm).

3.3. Spectral properties of MOCPc complexes in the presence of BSA

Fig. 3 shows the electronic absorption spectrum of $(OH)_2$GeOCPc in the presence of BSA (which is representative for all the complexes). The spectrum is slightly red shifted by about 3 nm, suggesting that the MOCPc complexes bind to BSA. The peak at 280 nm in Fig. 3, is due to BSA absorption. The MOCPcs in solution with BSA are monomeric irrespective of the serum protein concentration. Fluorescence spectra of the MOCPcs (Fig. 4 for (OH)AlOCPc) indicate that the fluorescence of these species are slightly quenched in the presence of BSA. Such quenching has been observed before for aluminium sulfonated phthalocyanine ($AlPcS_1$) in the presence of human serum albumin [29]. Fig. 3 shows that the MOCPc molecules form ground state complexes with BSA, thereby resulting in static fluorescence quenching. There was a slight decrease in the Φ_F values of all the MOCPcs in the presence of BSA, Table 1.

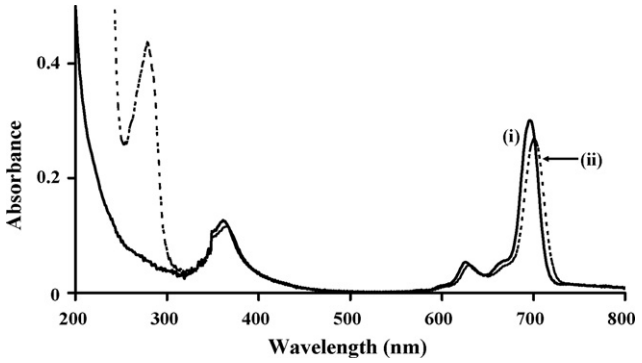

Fig. 3. UV–vis absorption spectra of $(OH)_2$GeOCPc alone (solid line) (i) and $(OH)_2$GeOCPc in the presence of BSA (dotted line) (ii) showing a shift on addition of BSA ([$(OH)_2$GeOCPc] = 4.1×10^{-6} mol dm^{-3}, [BSA] = 3×10^{-5} mol dm^{-3}).

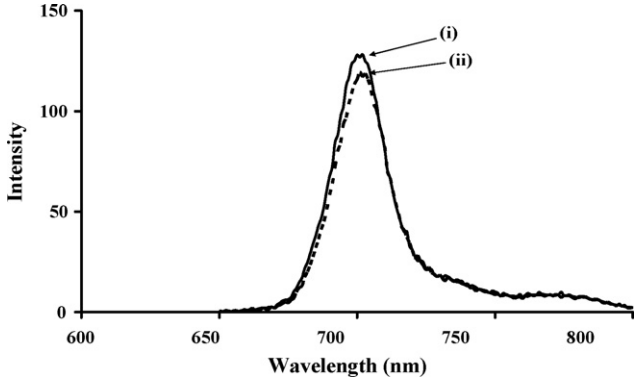

Fig. 4. Fluorescence emission spectra of (OH)AlOCPc in the presence and absence of BSA. (i) [(OH)AlOCPc] = 1.1×10^{-6} mol dm^{-3}; (ii) [BSA] = 3×10^{-5} mol dm^{-3}) (λ_{exc} = 640 nm).

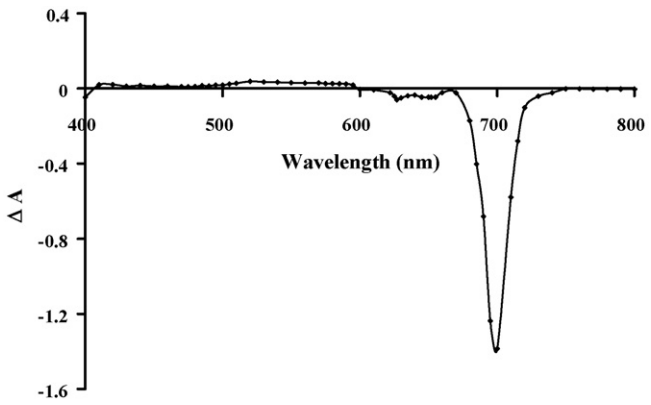

Fig. 5. Transient absorption spectrum of (OH)AlOCPc (~8.2×10^{-6} mol dm^{-3}) in the presence of BSA (3×10^{-5} mol dm^{-3}).

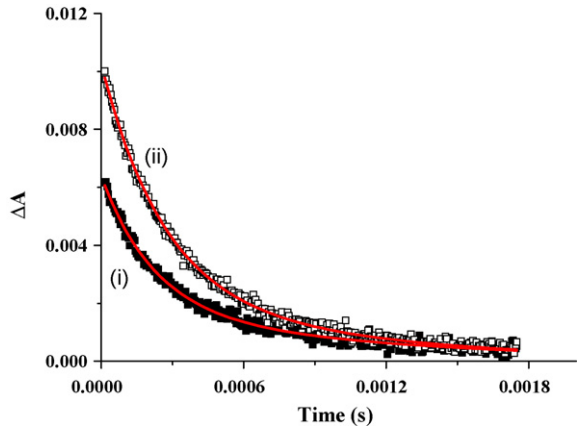

Fig. 6. Triplet decay curve for (i) ZnOCPc and (ii) ZnOCPc in the presence of BSA.

Decreased Φ_F values have been observed before for non-aggregated sulfonated MPcs in the presence of BSA [17].

The Φ_T values in the presence of BSA in Table 1 suggest that the BSA binding slightly reduces the Φ_T of the species, though not significantly, except for $(OH)_2$SiOCPc where there was a slight increase. The transient absorption spectra of the MOCPcs in the presence of BSA closely resemble those obtained in the absence of BSA as shown in Fig. 5 (for (OH)AlOCPc). The triplet curve in Fig. 6 obeyed second order kinetics. This is typical of MPc complexes at high concentrations (> 1×10^{-5} M) [30] due to the triplet–triplet recombination. The concentrations employed in this work were in this range hence triplet–triplet recombination is expected.

Triplet state lifetimes (τ_T) of the MOCPcs in the presence of BSA are longer than those of the MOCPc complexes in the absence of BSA. This observation could be due to the fact that there is a reduction in the exposure of the phthalocyanine to the aqueous medium because of the presence of the serum proteins.

Φ_Δ values were found to be higher in the presence of BSA. The efficiency of singlet oxygen generation should depend on the triplet state quantum yield and lifetime and the efficiency of energy transfer from the excited triplet state. The fact that higher Φ_Δ values were observed in the presence of BSA may be due to an efficient quenching of the triplet state by oxygen in the presence of BSA, as a result of the increased lifetime of the triplet state of the MOCPcs in the presence of BSA, Table 1.

Photodegradation quantum yields (Φ_{Pd}) of the MPc complexes increased in the presence of BSA, and this can be attributed to the fact that there may be formation of active oxidative albumin species (Scheme 1) since singlet oxygen generation of the MOCPcs is increased in the presence of BSA and these oxidative species could add to the photodegradation of the MPc complexes in the presence of BSA. Singlet oxygen is known to have the ability to react with

$$\text{MPc} + \text{BSA} \longrightarrow \text{MPc - BSA} \quad \text{(i)}$$

$$\text{MPc - BSA} \xrightarrow{h\nu} \text{*MPc - BSA} \quad \text{(ii)}$$

$$\text{*MPc - BSA} + {}^3O_2 \longrightarrow \text{MPc - BSA} + {}^1O_2 \quad \text{(iii)}$$

$$\text{MPc - BSA} + {}^1O_2 \longrightarrow \text{MPc} + \text{BSA oxidation products} \quad \text{(iv)}$$

Scheme 1. Photosensitized oxidation of BSA in the presence of MPc.

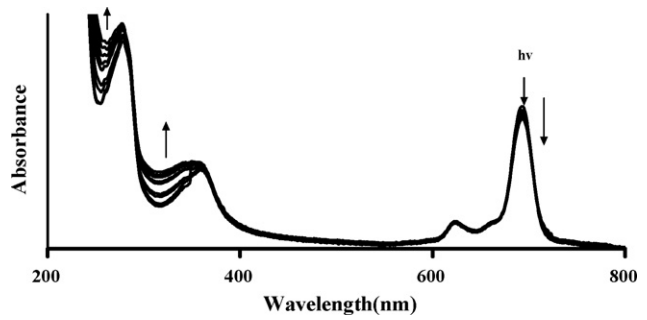

Fig. 7. Photolysis of (OH)AlOCPc in the presence of BSA showing the spectral changes observed at irradiation time interval of 5 min. Light intensity = 3.12×10^{16} photons s^{-1} cm^{-1} ([(OH)AlOCPc] = 5.5×10^{-6} M and BSA = 3×10^{-5} M).

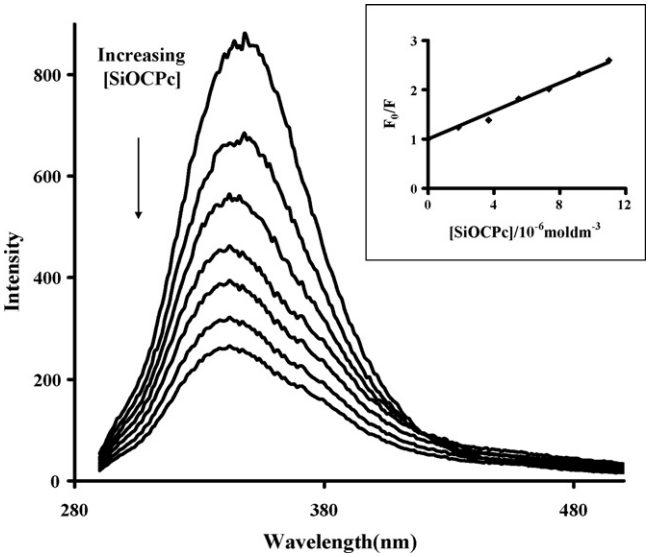

Fig. 8. Effect of MPc on fluorescence spectrum of BSA ([BSA] = 3.0×10^{-5} mol dm^{-3} [$(OH)_2$SiOCPc] = 0–1.10×10^{-5} mol dm^{-3}. Inset: Stern–Volmer plot for $(OH)_2$SiOCPc quenching of BSA.

macrocyclic metal complexes [28]. Fig. 7 shows the photodegradation spectra of (OH)AlOCPc in the presence of BSA with an increase in the 280 and 350 nm region, strengthening the fact that there are oxidation products of BSA formed.

3.4. Interaction of MPcs with BSA

3.4.1. Binding constants and fluorescence quenching

Fig. 8 shows the fluorescence emission spectra of BSA at a concentration of 3.0×10^{-5} M in the presence of varying concentrations of the respective MPc solution (0–1.10×10^{-5} mol dm^{-3}). BSA was excited at 280 nm and fluorescence recorded between 290 and 500 nm. There was a steady decrease in the intrinsic fluorescence of tryptophan residues in BSA with increase in MOCPc concentration, which can be attributed to fluorescence quenching. Fluorescence quenching can result from a variety of interactions such as excited state reactions, energy transfer, ground state complex formation or collisional quenching. The changes in BSA fluorescence intensity were related to the concentrations of the MOCPcs by the Stern–Volmer's relationship as given in Eq. (6) [31].

$$\frac{F_0^{BSA}}{F^{BSA}} = 1 + K_{SV}^{BSA}[\text{MPc}] \quad (6)$$

and K_{SV}^{BSA} is given by Eq. (7):

$$K_{SV}^{BSA} = k_q \tau_F^{BSA} \quad (7)$$

where F_0^{BSA} and F^{BSA} are the fluorescence intensities of BSA in the absence and presence of MPcs, respectively; K_{SV}^{BSA}, the Stern–Volmer quenching constant; k_q, the bimolecular quenching constant; and τ_F^{BSA}, the fluorescence lifetime of BSA. τ_F^{BSA} is known to be 10 ns, [32,33] thus, from the values K_{SV}^{BSA} obtained from the plots of F_0^{BSA}/F^{BSA} versus [MPc], the value of k_q may be determined (Eqs. (6) and (7)).

The inset in Fig. 8 shows the Stern–Volmer plot which indicates that within the investigated range of concentrations, the results agree with the Stern–Volmer equation. K_{SV}^{BSA} were determined from the slopes of these plots with respect to individual MPcs. The K_{SV} values determined are static quenching constants since there is a formation of a ground state complex between the MPcs and BSA as shown from their ground state absorption spectra in Fig. 3. Table 2 shows that the K_{SV} values of the silicon and germanium complexes are smaller than those of zinc and aluminium complexes, suggesting that the BSA fluorescence quenching with $(OH)_2$SiOCPc and $(OH)_2$GeOCPc may not be as effective as that of (OH)AlOCPc and ZnOCPc, due to some steric hindrance that may result from the axial ligands of the former complexes. (OH)AlOCPc also has an axial ligand, but it shows higher K_{SV} values compared to ZnOCPc.

Using Eq. (7) and the approximate values of fluorescence lifetime of BSA (10 ns) [32,33], the bimolecular quenching constants (k_q) were determined for the individual MPcs. As shown in Table 2, the k_q values are higher (being in the order of 10^{13} dm^3 mol^{-1} s^{-1}) than the proposed value for dynamic quenching (10^{10} dm^3 mol^{-1} s^{-1}) [34] indicating that quenching mechanism in this case is static. k_q values reported in this work are within the same order of magnitude as the values obtained for tetrasulfonated metallophthalocyanines (TSPcs); GeTSPc and SiTSPc [35].

The spectral changes in Fig. 3 indicate that the complexes bind to BSA, hence the fluorescence quenching experiment in Fig. 8 was used to estimate the binding constants (k_b) and the number of binding sites (n) using Eq. (8) [36,37].

$$\log\left[\frac{(F_0 - F)}{(F - F_\infty)}\right] = \log k_b + n \log[\text{MPc}] \quad (8)$$

where F_0 and F are the fluorescence intensities of BSA in the absence and presence of MPcs respectively; F_∞, the fluorescence intensity of BSA saturated with MPc; k_b, the binding constant; n, the number of binding sites on a BSA molecule; and [MPc] the concentration of different MPc. Plots of $\log[(F_0 - F)/(F - F_\infty)]$ against log[MPc] provide the values of n (from slope) and k_b (from the intercept).

Table 2
Quenching and binding data for the interaction of MPcs with BSA.

	K_{SV}^{BSA} (10^{-5} M^{-1})	R^a	k_q (10^{-13} M^{-1} s^{-1})	k_b (10^{-6} dm^3 mol^{-1})	n
(OH)AlOCPc	1.78	0.99	1.78	2.24	1.2
ZnOCPc	1.75	0.98	1.75	8.52	1.3
$(OH)_2$SiOCPc	1.42	0.99	1.42	0.27	1.1
$(OH)_2$GeOCPc	1.62	0.99	1.62	0.57	1.1

[a] R is correlation coefficient.

The values of k_b and n are characteristic of MPc–BSA interactions in aqueous medium [37], Table 2. The values indicate that all the complexes bind readily to BSA since serum albumins have high affinities for negatively charged molecules [38]. The k_b values for $(OH)_2$SiOCPc and $(OH)_2$GeOCPc) are lower than those reported for GeTSPc ($k_b = 2.38 \times 10^7$ dm^3 mol^{-1}) and SiTSPc ($k_b = 3.02 \times 10^7$ dm^3 mol^{-1}) [35], due to their monomeric nature, suggesting that MOCPcs bind to BSA less efficiently when compared to the tetrasulfonated derivatives. The k_b values for the silicon and germanium complexes are again lower than those of zinc and aluminium complexes which may be due to the steric hindrance of axial ligands which does not allow the full exposure of the MPcs to the protein environment. This shows that there is some agreement between k_b and K_{SV}. The number of binding sites in these experiments is ~1 suggesting a 1:1 stoichiometry for all the MPcs and BSA, as was the case for MTSPc complexes [35].

4. Conclusions

The photophysical and photochemical properties of MOCPc complexes in aqueous medium and in the presence of BSA have been studied. The MOCPcs exhibited increased efficiency of singlet oxygen generation via energy transfer from the excited triplet state in the presence of BSA. The triplet state lifetimes of the MOCPcs increased in the presence of BSA. The large binding constants suggest that the MOCPc complexes strongly interact with BSA; hence they can be easily transported in the blood. The probable mechanism of quenching of BSA fluorescence by the MOCPcs is static quenching.

Acknowledgements

This work was supported by the Department of Science and Technology (DST) and National Research Foundation (NRF), South Africa through DST/NRF South African Research Chairs Initiative for Professor of Medicinal Chemistry and Nanotechnology as well as Rhodes University and Medical Research Council of South Africa. MI thanks the Andrew Mellon Foundation for a scholarship.

References

[1] R. Bonnett, Chem. Soc. Rev. (1995) 19.
[2] S.B. Brown, E.A. Brown, I. Walker, Lancet Oncol. 5 (2004) 497.
[3] D.E.J.G.J. Dolmans, D. Fukumura, R.K. Jain, Nat. Rev. Cancer 3 (2003) 380.
[4] R. Bonnett, Chemical Aspects of Photodynamic Therapy, Gordon and Breach Science Publishers, Amsterdam, 2000.
[5] C.M. Allen, W.M. Sharman, J.E. van Lier, J. Porphyrins Phthalocyanines 5 (2001) 161.
[6] J.D. Spikes, Photochem. Photobiol. 43 (1986) 691.
[7] J.D. Spikes, J. Photochem Photobiol. B: Biol. 6 (1990) 259.
[8] T. Nyokong, Coord. Chem. 251 (2007) 1707.
[9] S.B. Kahl, J. Li, Inorg. Chem. 35 (1996) 3878.
[10] M.P. de Filippis, D. Dei, L. Fantetti, G. Roncucci, Tetrahedron Lett. 41 (2000) 9143.
[11] U. Kragh-Hansen, Pharmacol. Rev. 33 (1981) 17.
[12] T. Tanaka, S. Shiramoto, M. Miyashita, Y. Fujishima, Y. Kaneo, Int. J. Pharm. 277 (2004) 39.
[13] D.C. Carter, J.X. Ho, Adv. Protein Chem. 45 (1994) 153.
[14] A.A. Bhattacharya, S. Curry, N.P. Franks, J. Biol. Chem. 275 (2000) 38731.
[15] G. Jori, in: B.W. Henderson, T.J. Dougherty (Eds.), Photodynamic therapy basic principles and clinical applications, Marcel Dekker, New York, NY, 1992.
[16] J.D. Huang, S. Wang, P.C. Lo, W.P. Fong, W.H. Ko, D.K.P. Ng, New J. Chem. 28 (2004) 348.
[17] A. Ogunsipe, T. Nyokong, Photochem. Photobiol. Sci. 4 (2005) 510.
[18] K. Ozoemena, N. Kuzetnova, T. Nyokong, J. Photochem, Photobiol. A: Chem. 139 (2001) 217.
[19] K. Sakamoto, E. Ohno, Prog. Org. Coat. 31 (1997) 139.
[20] J.H. Weber, D.H. Busch, Inorg. Chem. 4 (1965) 469.
[21] A.O. Ogunsipe, T. Nyokong, J. Photochem. Photobiol. A: Chem. 173 (2005) 211.
[22] S. Fery-Forgues, D. Lavabre, J. Chem. Ed. 76 (1999) 1260.
[23] A. Ogunsipe, J.Y. Chen, T. Nyokong, New J. Chem. 7 (2004) 822.
[24] A. Harriman, M.C. Richoux, J. Chem. Soc., Faraday Trans. 276 (1980) 1618.
[25] I. Seotsanyana-Mokhosi, N. Kuznetsova, T. Nyokong, J. Photochem. Photobiol. A: Chem. 140 (2001) 215.
[26] F. Wilkinson, W.P. Helman, A.B. Ross, J. Phys. Chem. Ref. Data 22 (1993) 113.
[27] M.J. Stillman, T. Nyokong, in: C.C. Leznoff, A.B.P. Lever (Eds.), Phthalocyanines: Properties and Applications, vol. 1, VCH Publishers, New York, 1989 (Chapter 3).
[28] G. Schnurpfeil, W. Spiller, H. Kliesch, D. Worhle, J. Porphyrins Phthalocyanines 1 (1997) 159.
[29] M.S.C. Foley, A. Beeby, A.W. Parker, S.M. Bishop, D. Phillips, J. Photochem. Photobiol. B: Biol. 38 (1997) 10.
[30] M.G. Debacker, O. Deleplanque, B. Van Vlierberge, F.X. Sauvage, Laser Chem. 8 (1988) 1.
[31] J. Rose, Advanced Physico-chemical Experiments, first ed., Sir Isaac Pitman and Sons Ltd., London, 1964, p. 257.
[32] M. Guo, J.W. Zou, P.G. Yi, Z.C. Shang, G.X. Hu, Q.S. Yu, Anal. Sci. 20 (2004) 465.
[33] J.R. Lakowicz, G. Weber, Biochemistry 12 (1973) 4161.
[34] S.L. Murov, I. Carmichael, G.L. Hug, Handbook of Photochemistry, second ed., Decker M, New York, 1993, 207.
[35] M. Idowu, T. Nyokong, J. Photochem. Photobiol. A: Chem. 197 (2008) 273.
[36] D.M. Chipman, V. Grisaro, N. Sharon, J. Biol. Chem. 242 (1967) 4388.
[37] S.M.T. Nunes, F.S. Squilla, A.C. Tudesco, Braz. J. Med. Biol. Res. 37 (2004) 273.
[38] A.I. Filyasova, I.A. Kudelina, A.V. Feofanov, J. Mol. Struct. 565–566 (2001) 173.